

Water-induced superconductivity in SrFe₂As₂

Hidenori Hiramatsu,^{1,*} Takayoshi Katase,² Toshio Kamiya,^{1,2} Masahiro Hirano,^{1,3} and Hideo Hosono^{1,2,3}
¹ERATO–SORST, Japan Science and Technology Agency, in Frontier Research Center, Tokyo Institute of Technology, S2-6F East,
 Mailbox S2-13, 4259 Nagatsuta-cho, Midori-ku, Yokohama 226-8503, Japan

²Materials and Structures Laboratory, Tokyo Institute of Technology, Mailbox R3-1, 4259 Nagatsuta-cho, Midori-ku,
 Yokohama 226-8503, Japan

³Frontier Research Center, Tokyo Institute of Technology, S2-6F East, Mailbox S2-13, 4259 Nagatsuta-cho, Midori-ku,
 Yokohama 226-8503, Japan

(Received 18 May 2009; revised manuscript received 3 July 2009; published 10 August 2009)

It has been considered that FeAs-based high-transition temperature (high- T_c) superconductors need electron or hole doping by aliovalent-ion substitution or large off stoichiometry in order to induce superconductivity. We report that exposure of undoped SrFe₂As₂ epitaxial thin films to water vapor induces a superconducting transition. These films exhibit a higher onset T_c (25 K) and larger magnetic field anisotropy than those of cobalt-doped SrFe₂As₂ epitaxial films, suggesting that the mechanism for the observed superconducting transition differs from that of the aliovalent-ion-doped SrFe₂As₂. The present finding provides an interesting approach to induce superconductivity with a higher T_c in FeAs-based superconductors.

DOI: 10.1103/PhysRevB.80.052501

PACS number(s): 74.70.Dd, 74.62.Bf, 74.62.Yb

Discovery of an Fe-based layered superconductor, F-doped LaFeAsO rekindled extensive researches on superconducting materials.¹ Since then, four types of material systems have been known to be superconductors, which are ReFeAsO (Re =rare earths),^{1–3} AeFe₂As₂ (Ae =alkaline earths),⁴ AFeAs (A =alkali metal),⁵ and FeSe (Ref. 6) phases, and the maximum transition temperature (T_c) has reached 56 K in Th-doped GdFeAsO.³ Each of the Fe-based compounds has layered crystal structures that possess FeAs (or FeSe) layers composed of edge-sharing FeAs₄ (FeSe₄) tetrahedra, implying that the two dimensionality and the local FeAs (FeSe) structures play an important role in inducing the superconductivity. Mostly, undoped parent phases of these materials exhibit structural phase transitions, which accompany antiferromagnetic ordering transitions, at low temperatures, but do not exhibit superconductivity at least down to 2 K.^{6–10} Carrier doping by aliovalent-ion substitution^{1–4,11–13} or introducing off stoichiometry^{5,6,14,15} suppresses the structure and magnetic transitions and induces superconductivity. In addition to the carrier doping, high-pressure-induced superconductivity have been reported in AeFe₂As₂.^{16–21} Further, there has been one report on ambient-pressure superconductivity on nominally undoped AeFe₂As₂ (Ref. 22); however, it is considered that the superconductivity in the nominally undoped cases is caused by lattice distortion in their SrFe₂As₂ crystals. These results indicate that superconductivity in AeFe₂As₂ is sensitive to an external stress, a sample preparation condition, and a post-treatment condition; it in turn suggests that we may find a different approach to attain high- T_c superconductivity in the FeAs-based compounds.

In this Brief Report, we report on a different type of superconducting transition in undoped SrFe₂As₂ in which exposure of SrFe₂As₂ epitaxial thin films to water vapor invokes a superconducting transition at an onset transition temperature (T_c^{onset}) of 25 K. It would be worth noting that water-intercalated superconductivity is known in some layered crystals such as A_x(H₂O)_yTS (A =Na, K, Rb, and Cs; T =Nb and Ta; T_c =5.5 K),²³ Na_xCoO₂·yH₂O (T_c =5 K),²⁴ and Na_x(H₂O)_y(MS)_{1+δ}(TaS₂)₂ (M =Sn, Pb, and Sb; T_c =4 K).²⁵ These are explained by enhanced two dimension-

ality in connection with the expansion of the interlayer distances induced by the water intercalation. On the contrary, the SrFe₂As₂ epitaxial films exhibit the superconducting transition although the interlayer distance (i.e., the c -axis length of the unit cell) is shrunken by the exposure to water vapor. In addition, the T_c and the superconductivity anisotropy are different largely from aliovalent-ion-doped SrFe₂As₂. These discrepancies imply that a different mechanism controls the emergence of the superconducting transition in SrFe₂As₂ by water exposure.

Epitaxial thin films of undoped SrFe₂As₂ (thickness ~200 nm) were grown on mixed perovskite (La,Sr)(Al,Ta)O₃ (001) single-crystal substrates by pulsed laser deposition^{26,27} using undoped SrFe₂As₂ sintered disks as the targets at the substrate temperature of ~700 °C in vacuum of ~10⁻⁵ Pa. Crystalline quality and orientation were examined by high-resolution x-ray diffraction (XRD, radiation: Cu $K\alpha_1$ and apparatus: ATX-G, Rigaku). We confirmed that the intensity and width of diffraction peaks and rocking curves, which are the measure of the crystalline quality and orientation, were comparable to those of the epitaxial films of cobalt-doped SrFe₂As₂ that exhibited superconducting transitions at $T_c^{\text{onset}}=20$ K.²⁷ Resistivity (ρ)-temperature (T) curves were measured using a physical properties measurement system (Quantum Design) in a vacuum from 2 to 300 K under external magnetic fields (H) varied up to 9 T.

The solid line in Fig. 1(a) shows the ρ - T curve of the virgin SrFe₂As₂ epitaxial film, which was measured immediately after taken out from the deposition chamber. A resistivity anomaly corresponding to a structural phase transition and an antiferromagnetic ordering is observed at $T_{\text{anom}}=204$ K, which is almost the same as those reported previously for undoped bulk samples.^{28,29} No superconducting transition is observed for the virgin film. On the other hand, after exposing the virgin film to an ambient atmosphere at room temperature with the relative humidities of 40–70 RH% for 2 h, ρ started dropping at 25 K [the dashed line in Fig. 1(a) and the triangles in Fig. 1(b)]. With increasing the exposure time, the drop of ρ became sharper and finally the

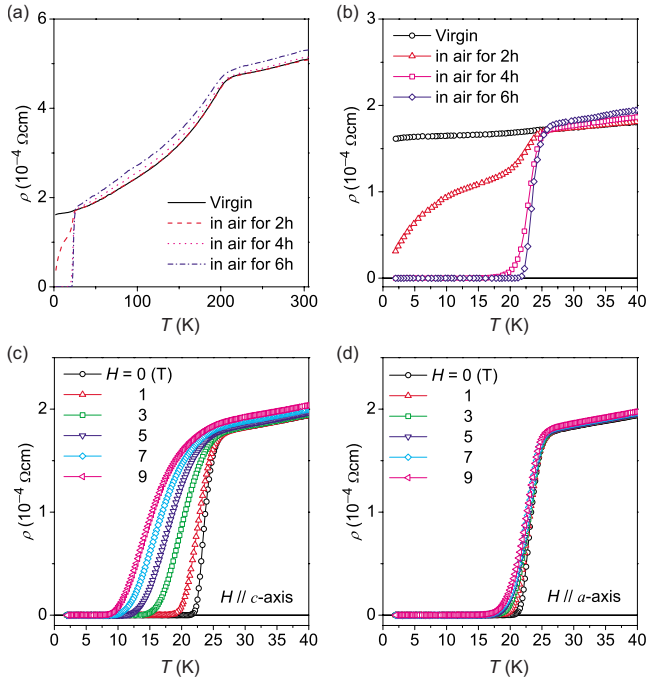


FIG. 1. (Color online) (a) Variation in ρ - T curves as a function of air-exposure time for SrFe₂As₂ epitaxial films as grown (virgin, solid line), exposed to air for 2 h (dashed line), 4 h (dotted line), and 6 h (dotted-dashed line). (b) Extended view of (a) between 2 and 40 K. [(c) and (d)] Anisotropy of superconducting transition of the film exposed to air for 6 h under magnetic fields parallel to the (c) c axis ($H_{||c}$) and (d) a axis ($H_{||a}$) at $H_{||c,a}$ from 0 to 9 T.

zero resistance was observed at the exposure time ≥ 4 h. The T_c^{onset} and the offset T_c of the film exposed to air for 6 h (hereafter, referred to as the air-exposed film) are 25 and 21 K, respectively, which are higher by ~ 5 K than those of cobalt-doped SrFe₂As₂ epitaxial films.²⁷ These observations strongly suggest that a constituent in an ambient air induces the superconducting transition in SrFe₂As₂.

Figures 1(c) and 1(d) show magnetic anisotropy of the air-exposed film. T_c was shifted to lower temperatures with increasing H for both the H directions parallel to the c axis ($H_{||c}$) and the a axis ($H_{||a}$). Superconducting transitions survived at ≤ 7 K for $H_{||c}$ and ≤ 16 K for $H_{||a}$ even when H was raised up to 9 T, indicating that the upper critical magnetic fields are far above 9 T. It is observed that T_c is more sensitive to the $H_{||c}$ than to the $H_{||a}$. It would be worth noting that the large anisotropy of T_c in the air-exposed SrFe₂As₂ epitaxial films is rather different from that of the cobalt-doped SrFe₂As₂ epitaxial films reported in Refs. 27 and 30, which showed almost isotropic behaviors; the large anisotropy is more similar to that reported for the ReFeAsO system.³¹

Figure 2(a) shows out-of-plane XRD patterns around the SrFe₂As₂ 002 diffraction. It shows that exposure to air for 6 h broadened and upper shifted the SrFe₂As₂ 002 diffraction peak. It accompanies formation of a small amount of an Fe₂As impurity phase, which is confirmed by an additional broad peak at $2\theta \sim 14.9^\circ$. This observation indicates that the c -axis length of the SrFe₂As₂ phase was decreased from 1.233 nm in the virgin film [this value is slightly smaller (-0.4%) than that of bulk SrFe₂As₂, 1.238 nm (Ref. 28)] to

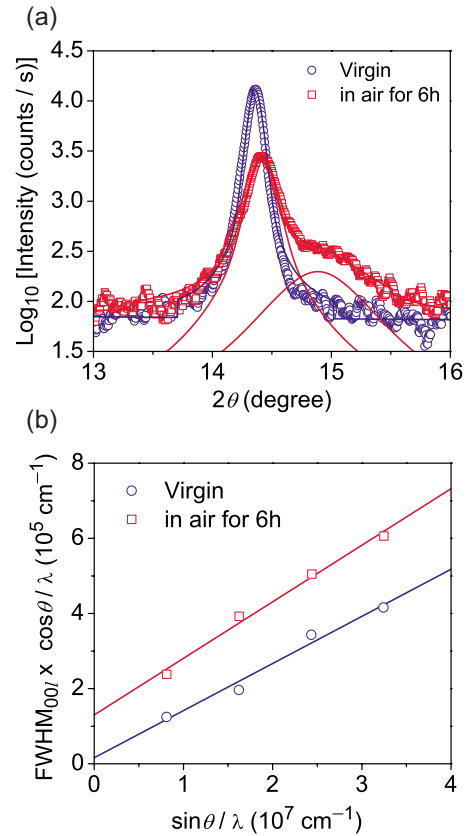


FIG. 2. (Color online) (a) ω -coupled 2θ scan XRD patterns around 002 diffraction of SrFe₂As₂ epitaxial films at room temperature. The circles and squares show the virgin film and the film exposed to air for 6 h, respectively. The lines are the deconvolution of the XRD patterns. (b) Williamson-Hall plots of $00l$ diffractions.

1.227 nm in the air-exposed film. The latter value is slightly smaller even than that of the cobalt-doped SrFe₂As₂ epitaxial films [$c = 1.230$ nm (Ref. 27)]. This shrinkage would be related to the superconducting transition because it has been reported that applying a high pressure to undoped SrFe₂As₂ invokes superconducting transitions.^{17–21} In those cases, T_c^{onset} reaches ca. 35–38 K and T_{anom} shifts to lower temperatures as the external pressure increases. On the other hand, in the present case, the shift of T_{anom} is not observed as seen in Fig. 1(a) and the observed T_c are lower than the maximum T_c of the pressure-induced cases, which is similar to more recent report that no T_{anom} shift is observed in the pressure-induced superconduction.²¹ Figure 2(b) shows the Williamson-Hall plots of the full width at half maximum (Δ) for the $00l$ diffractions of the SrFe₂As₂ films, which corresponds to the relation $\Delta \cdot \cos\theta / \lambda = K(D^{-1} + 2\eta \cdot \sin\theta / \lambda)$, where θ denotes the diffraction angle, K the constant (0.9 for a Gaussian peak profile), D the height of the single-domain crystallite, λ the wavelength of x ray, and η the inhomogeneous strain.³² The slope (2η) was not changed largely by the air exposure, indicating the major origin of the peak broadening is not the internal inhomogeneity in the crystalline lattice, which is often induced by lattice strain and impurity incorporation. The slight change in the slope, however, can be related to the superconductivity in the case of strain-induced superconductivity discussed in Refs. 17, 21,

and 22. The intercepts at the vertical axis in Fig. 2(b) provide the crystallite heights D , which were estimated to be 680 nm for the virgin film and 80 nm for the air-exposed film. The former value overestimates the crystallite height because the film thickness is thinner, 190 nm. This value is, however, reasonable because the intersect value approaches zero for a larger crystallite size in the Williamson-Hall plot, which gives a larger error. Therefore, this result indicates that the crystallites in the virgin film are single domain in height. The value of the crystallite height for the air-exposed film is more accurate because the intersect value is much larger than zero, and the obtained crystallite size (80 nm) is consistent with the film thickness (190 nm). It safely concludes the air exposure decreased the crystallite height, which is the major origin of the broadening in the diffraction peak discussed above. It is possible to estimate the change in the volume of the SrFe_2As_2 phase by comparing integrated diffraction intensities of the SrFe_2As_2 002 diffractions, which were estimated from the intensities and widths of the diffraction peaks and the rocking curve peaks. We observed that the air exposure reduced the peak intensity to $\sim 20\%$ and increased the width of the diffraction peak to 190% and that of the rocking curve to 120% of those of the virgin film, which indicates that the volume of the SrFe_2As_2 phase in the air-exposed film is decreased to 46% of the virgin film. This volume change corresponds reasonably to the ratio of the residual crystallite height (80 nm) and the film thickness (190 nm), suggesting that the vertical single-domain structure is maintained in the SrFe_2As_2 phase even after the air exposure. By contrast, the volume fraction of the Fe_2As phase was estimated to be $\sim 10\%$ of the SrFe_2As_2 phase from the integrated peak area and the structure factors of these diffractions. These results substantiate that SrFe_2As_2 is the majority phase even after the air exposure.

To determine the origin of the appearance of the superconducting transition induced by the air exposure, we investigated the effects of exposure to the air constituents separately (Fig. 3). Exposure to a dry nitrogen gas (purity: 6N, dew point: $\leq -80^\circ\text{C}$, and pressure: 300 Torr) for 24 h at room temperature did not induce any change [Fig. 3(a)], proving that dry N_2 is inert for undoped SrFe_2As_2 films at least at room temperature. Exposure to a dry oxygen gas (6N, $\leq -80^\circ\text{C}$, and 300 Torr) and a dry carbon dioxide gas (4N, $\leq -76^\circ\text{C}$, and 760 Torr) for 24 h at room temperature [Figs. 3(b) and 3(c)] gave small changes in the ρ values but did not induce a superconducting transition at least down to 2 K. The small increase in ρ in the dry oxygen gas and the small decrease in the dry carbon dioxide gas suggest some doping effects by these molecules. Figure 3(d) shows the effect of water vapor (a dew point was $+13^\circ\text{C}$, 760 Torr, generated from distilled water with a dry nitrogen gas as a carrier gas). A clear superconducting transition was observed at $T_c^{\text{onset}} = 25$ K, which is the same temperature as that of the air-exposed film. Therefore, we conclude that the superconducting transition is induced by exposure to H_2O -related species to the SrFe_2As_2 films. As clarified by the XRD study, the exposure to H_2O -related species accompanies the shrinkage of the c -axis length of the SrFe_2As_2 lattice and the appearance of the Fe_2As phase. The effect of the Fe_2As phase is excluded from the origin of the superconducting transition

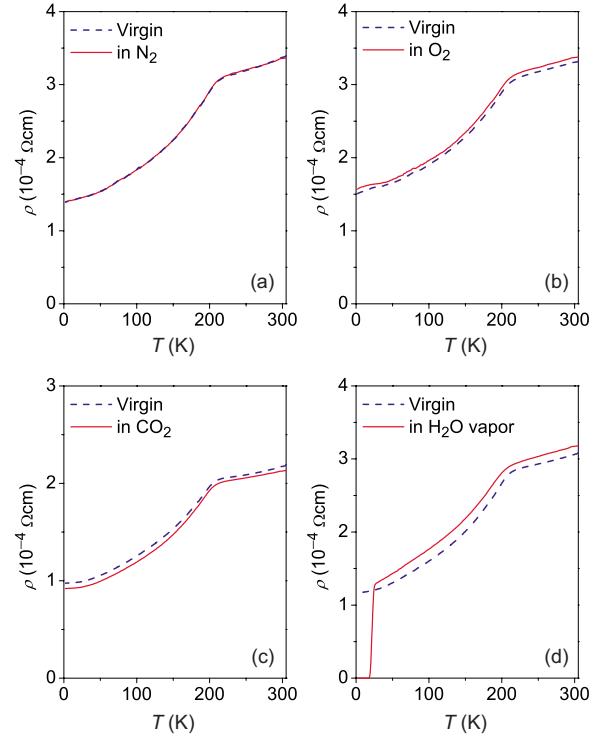


FIG. 3. (Color online) Changes in ρ - T curves of SrFe_2As_2 epitaxial films under exposure to various atmospheres. The dashed lines show the data of the virgin films and the solid lines show those of the films exposed to (a) dry nitrogen for 24 h, (b) dry oxygen for 24 h, (c) dry carbon dioxide for 24 h, and (d) water vapor (the dew point = $+13^\circ\text{C}$) for 2 h.

because no superconducting transition has been reported for Fe_2As [reported to be an antiferromagnet with the Néel temperature of 353 K (Ref. 33)] as far as we know. Therefore, we consider that the shrinkage of the c axis would closely be related to the appearance of the superconducting transition.

The crystal structure^{29,34} in Fig. 4(a) tells that it has two large interstitial sites; one is the I_9 site surrounded by four

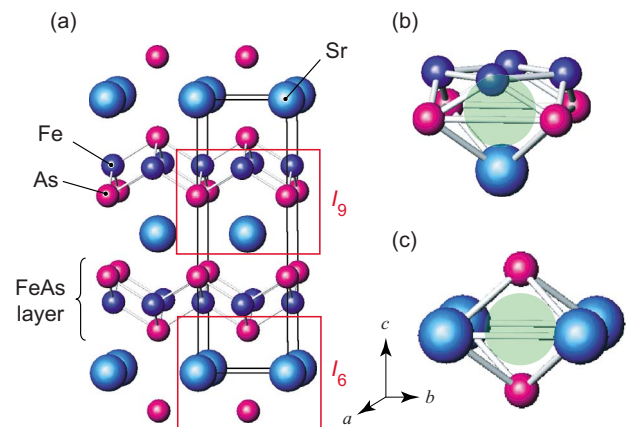


FIG. 4. (Color online) (a) Crystal structure of SrFe_2As_2 with ThCr_2Si_2 -type structure. The box indicates the unit cell. [(b) and (c)] Expanded views of the interstitial sites. (b) I_9 , which is surrounded by four As, four Fe, and one Sr, and (c) I_6 , which is surrounded by four Sr and two As.

As, four Fe, and one Sr [Fig. 4(b)] and the other the I_6 site surrounded by four Sr and two As [Fig. 4(c)] in which the sizes of the free spaces (0.15 nm in the a - b planes) are close to that of an O^{2-} ion (0.14 nm). Preliminarily first-principles structure relaxation calculations³⁵ showed that incorporation of an H_2O molecule at the I_9 or I_6 sites formed quantum-mechanically (meta-) stable structures but it moved the molecule from the interstitial sites to interlayer sites and expanded the c -axis length significantly, which is similar to the intercalation cases such as $A_x(H_2O)_yTS$, $Na_xCoO_2 \cdot yH_2O$, and $Na_x(H_2O)_y(MS)_{1+\delta}(TaS_2)$ (Refs. 23–25); it is inconsistent with the observed shrinkage of the c -axis length observed above. Incorporation of an OH or an oxygen atom at the I_9 site or the I_6 site found the stable positions at the symmetric positions near the centers of the coordination polyhedra. Those at the I_9 site did not expand the c axis largely (the expansion in the c -axis length is as small as 0.01 nm for the oxygen case) while the latter expanded it by 0.10 nm because the interatomic distance between the two As atoms are only 0.35 nm and is not large enough to incorporate an oxygen ion. These results suggest that the most probable case among them is the incorporation of oxygen atoms at the I_9 sites but any of these cases appears not to be able to explain the shrinkage of the c -axis length. Another possibility would be the formation of Sr vacancies by removing the Sr ions through a reaction, e.g., $SrFe_2As_2 + 2H_2O \rightarrow SrFe_2As_2:V_{Sr} + Sr(OH)_2 + H_2$, which may likely occur be-

cause an Ae element easily reacts with H_2O to form a hydroxide.

In summary, we have found that water vapor induces a superconducting transition in undoped $SrFe_2As_2$ epitaxial films at an ambient pressure. The T_c^{onset} was 25 K, which is higher than that of the cobalt-doped epitaxial films. The exposure to water vapor reduced the c -axis length of the $SrFe_2As_2$ phase as a primary effect. The induction of the superconductivity can be explained by the chemical pressure-induced consequently. In this Brief Report, it is concluded that the superconducting transition originates from the $SrFe_2As_2$ phase because $SrFe_2As_2$ is the major phase in the air-exposed film, T_c is higher but similar to those reported on cobalt-doped $SrFe_2As_2$, and no other superconducting phase was detected by the XRD measurements. However, we cannot exclude possibility that a subproduct of the reaction between the $SrFe_2As_2$ film and H_2O causes the superconducting transitions. Even though, such a case will lead to more interesting discovery because the remaining possible origins are Fe_2As , $FeAs$, and an amorphous phase that was not detected by XRD measurements but any of them has not been reported to be a superconductor. Although further study is needed to clarify the origin of the superconduction and/or the doping mechanism, the present finding provides not only an interesting insight into understanding superconducting transitions in undoped $AeFe_2As_2$ but also a clue to obtaining higher T_c by a doping method such as chemical modification.

*h-hirama@lucid.msl.titech.ac.jp

- ¹Y. Kamihara, T. Watanabe, M. Hirano, and H. Hosono, *J. Am. Chem. Soc.* **130**, 3296 (2008).
- ²X.-H. Chen *et al.*, *Nature (London)* **453**, 761 (2008).
- ³C. Wang *et al.*, *EPL* **83**, 67006 (2008).
- ⁴M. Rotter, M. Tegel, and D. Johrendt, *Phys. Rev. Lett.* **101**, 107006 (2008).
- ⁵X. C. Wang *et al.*, *Solid State Commun.* **148**, 538 (2008).
- ⁶F.-C. Hsu *et al.*, *Proc. Natl. Acad. Sci. U.S.A.* **105**, 14262 (2008).
- ⁷T. Nomura *et al.*, *Supercond. Sci. Technol.* **21**, 125028 (2008).
- ⁸C. de la Cruz *et al.*, *Nature (London)* **453**, 899 (2008).
- ⁹M. Rotter *et al.*, *Phys. Rev. B* **78**, 020503(R) (2008).
- ¹⁰Q. Huang *et al.*, *Phys. Rev. Lett.* **101**, 257003 (2008).
- ¹¹H. H. Wen *et al.*, *EPL* **82**, 17009 (2008).
- ¹²A. S. Sefat *et al.*, *Phys. Rev. B* **78**, 104505 (2008).
- ¹³A. Leithe-Jasper, W. Schnelle, C. Geibel, and H. Rosner, *Phys. Rev. Lett.* **101**, 207004 (2008).
- ¹⁴Z.-A. Ren *et al.*, *EPL* **83**, 17002 (2008).
- ¹⁵H. Kito, H. Eisaki, and A. Iyo, *J. Phys. Soc. Jpn.* **77**, 063707 (2008).
- ¹⁶M. S. Torikachvili, S. L. Bud'ko, N. Ni, and P. C. Canfield, *Phys. Rev. Lett.* **101**, 057006 (2008).
- ¹⁷M. S. Torikachvili, S. L. Bud'ko, N. Ni, and P. C. Canfield, *Phys. Rev. B* **78**, 104527 (2008).
- ¹⁸P. L. Alireza *et al.*, *J. Phys.: Condens. Matter* **21**, 012208 (2009).
- ¹⁹K. Igawa *et al.*, *J. Phys. Soc. Jpn.* **78**, 025001 (2009).
- ²⁰H. Kotegawa, H. Sugawara, and H. Tou, *J. Phys. Soc. Jpn.* **78**, 013709 (2008).
- ²¹E. Colombier, S. L. Bud'ko, N. Ni, and P. C. Canfield, *Phys. Rev. B* **79**, 224518 (2009).
- ²²S. R. Saha, N. P. Butch, K. Kirshenbaum, J. Paglione, and P. Y. Zavalij, *Phys. Rev. Lett.* **103**, 037005 (2009).
- ²³A. Lurf, F. Sernetz, W. Biberacher, and R. Schöllhorn, *Mater. Res. Bull.* **14**, 797 (1979).
- ²⁴K. Takada *et al.*, *Nature (London)* **422**, 53 (2003).
- ²⁵N. Katayama, M. Nohara, F. Sakai, and H. Takagi, *J. Phys. Soc. Jpn.* **74**, 851 (2005).
- ²⁶H. Hiramatsu, T. Katase, T. Kamiya, M. Hirano, and H. Hosono, *Appl. Phys. Lett.* **93**, 162504 (2008).
- ²⁷H. Hiramatsu, T. Katase, T. Kamiya, M. Hirano, and H. Hosono, *Appl. Phys. Express* **1**, 101702 (2008).
- ²⁸C. Krellner *et al.*, *Phys. Rev. B* **78**, 100504(R) (2008).
- ²⁹M. Tegel *et al.*, *J. Phys.: Condens. Matter* **20**, 452201 (2008).
- ³⁰S. A. Baily *et al.*, *Phys. Rev. Lett.* **102**, 117004 (2009).
- ³¹Y. Jia *et al.*, *Appl. Phys. Lett.* **93**, 032503 (2008).
- ³²G. K. Williamson and W. H. Hall, *Acta Metall.* **1**, 22 (1953).
- ³³H. Katsuraki and N. Achiwa, *J. Phys. Soc. Jpn.* **21**, 2238 (1966).
- ³⁴M. Pfisterer and G. Nagorsen, *Z. Naturforsch. B* **35**, 703 (1980).
- ³⁵Variable-cell relaxation calculations were performed based on the density-functional theory at the generalized gradient approximation $+U$ (GGA+ U) level using the VASP code [G. Kresse and J. Furthmüller, *Phys. Rev. B* **54**, 11169 (1996)] with a projector-augmented plane wave method; [P. E. Blöchl, *ibid.* **50**, 17953 (1994); G. Kresse and D. Joubert, *ibid.* **59**, 1758 (1999)] and PBE96 functionals.